

# Quantitative determination of polymorphic composition in intact compacts by parallel-beam X-ray powder diffractometry II Data correction for analysis of phase transformations as a function of pressure

Peter L.D. Wildfong<sup>a,\*</sup>, Nicole A. Morley<sup>b</sup>, Michael D. Moore<sup>b</sup>, Kenneth R. Morris<sup>b</sup>

<sup>a</sup> Duquesne University, Mylan School of Pharmacy, Department of Pharmaceutical Sciences, 600 Forbes Av., Pittsburgh, PA 15282, USA

<sup>b</sup> Purdue University Department of Industrial and Physical Pharmacy, 575 Stadium Mall Dr., West Lafayette, IN 47907, USA

Received 29 December 2004; received in revised form 10 March 2005; accepted 14 March 2005

Available online 24 May 2005

## Abstract

An analytical, non-destructive method using parallel-beam transmission powder X-ray diffractometry (PXRD) is presented for in situ whole compact detection and quantification of solid-state phase transformations in powder compacts. Accurate quantification of analyte in intact compacts using PXRD requires a mathematical correction prior to interpolation of calibration data to account for sample differences that result as a function of pressure; namely, compact thickness and solid fraction. Chlorpropamide is examined as a model system, selected because of its susceptibility to polymorphic transformations when consolidated using moderately low pressures. The results indicate that quantification of the transformed phase of chlorpropamide without corrections for solid fraction and thickness, underestimates the extent of transformation by 2.4%. Although the magnitude of the correction for this particular system of polymorphs is small, more significant values are expected for other compounds, particularly those with sufficient compactibility to allow the formation of low solid fraction calibration samples.

© 2005 Elsevier B.V. All rights reserved.

**Keywords:** Parallel-beam transmission PXRD; Phase transformation; Whole compact analysis; Polymorphs; Mechanical activation

## 1. Introduction

The new GMPs for the 21st century carry with them an increased focus on material and process understanding, both of which are essential for designing quality into pharmaceutical drug products. Within this context, the necessity of investigating sources of variation in the solid-state form of a drug is a key element of pharmaceutical product design as well as process control [1]. This undertaking follows the current industrial focus on better understanding the responses of pharmaceutical materials to manufacturing.

Powder X-ray diffraction (PXRD) is a convenient, non-destructive tool used to differentiate between multiple phases of materials, owing to the unique diffraction patterns

produced from the crystallographic structures of each polymorph. Traditional quantitative PXRD calibration data are generated from physical mixtures of powdered samples, which are easily prepared and mounted onto a standard diffractometer. Accurate quantification can be more complex for consolidated samples owing to geometry errors associated with traditional Bragg–Brentano reflectance mode applications [2,3], and signal attenuation due to sample densification [4]. For these reasons, PXRD phase quantification for consolidated samples is typically performed after compacts have been sectioned and reverted back into powders by trituration. This experimental approach may, however, be unacceptable for studying compounds in which mechanically activated phase transitions are suspected. Grinding materials during sample preparation can potentially induce further transformation [5–7], adding unwanted artifact to data. Accurate PXRD quantification of phase changes solely as a function

\* Corresponding author. Tel.: +1 412 396 1543 fax: +1 412 396 4660.

E-mail address: [wildfongp@duq.edu](mailto:wildfongp@duq.edu) (P.L.D. Wildfong).

of compaction is best accomplished using whole, intact compacts and employing suitable data corrections for the effects associated with the analysis of consolidated samples.

Thanks to recent advances in auxiliary PXRD equipment, standard laboratory instruments can be easily integrated with secondary optics capable of illuminating samples with more intense, nearly parallel-geometry incident beams, having the increased flux necessary for transmission through dense compacts. An example is the polycapillary optic (X-Ray Optical Systems, Albany, NY), which uses an array of fibrous glass tubes that collect X-rays from a standard point source. The X-rays are collimated into a quasi-parallel beam, which is emitted with a full-width at half maximum divergence of approximately  $0.2^\circ$  for Cu  $K\alpha$  wavelength radiation [8]. Illumination of samples with parallel beams eliminates the data artifacts associated with traditional Bragg–Brentano instrument configurations [2,3,9]. Recently, this setup was investigated and successfully employed for the study of intact compacts containing binary mixtures of polymorphs for two small molecular organic systems [3].

This paper extends our previously reported method for analysis of intact binary phase compacts to include the necessary corrections for samples prepared at various pressures. It was found that direct interpolation of standard calibration data will underestimate quantitative results; a problem easily eliminated by a simple mathematical correction, which allows the comparison of compacts prepared at different relative conditions (i.e. different pressures and/or dwell times).

## 2. Materials and methods

### 2.1. Preparation of pure samples of chlorpropamide polymorphs

Pure chlorpropamide form A (CPA-A) was obtained as a bulk crystalline powder from Sigma (Sigma Chemicals, St. Louis, MO). Pure samples of chlorpropamide form C (CPA-C) were prepared using a method similar to that reported by Simmons et al. [10]. Approximately 2.0 g samples of form A were placed in glass petri dishes, which were held at  $115^\circ\text{C}$  for 3 h in a Precision STM 80 mechanical convection oven (Precision Scientific, Winchester, VA). The phase purity of both forms was assessed by comparison of experimental powder X-ray diffraction patterns with patterns calculated from their respective crystal structures. Experimental and calculated PXRD data are shown in Fig. 1.

### 2.2. Powder X-ray diffraction analysis of chlorpropamide

All PXRD experiments were performed using a Shimadzu LabX XRD-6000 diffractometer (Kratos Analytical, Chestnut Ridge, NY) equipped with a Cu  $K\alpha$  anode ( $\lambda = 1.5406 \text{ \AA}$ ) and integrated with a polycapillary optic (XOS, Albany, NY).

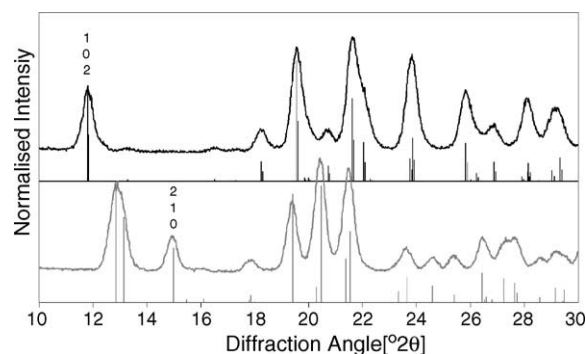


Fig. 1. Calculated diffraction patterns for CPA-A (black) and CPA-C (grey) compared with experimental data obtained from whole-compact transmission PXRD. The characteristic peaks used for quantification of forms A and C, respectively, occur at  $11.8^\circ 2\theta$  (corresponding to the 1 0 2 reflection) and  $15.0^\circ 2\theta$  (corresponding to the 2 1 0 reflection).

Diffraction data were collected at  $2^\circ/\text{min}$  using an angular step size of  $0.02^\circ 2\theta$ . The operational voltage and amperage were respectively set to 40.0 kV and 40.0 mA. Analyses of chlorpropamide compacts were performed in transmission mode using a custom aluminum sample holder through which a 0.5 in. diameter hole was bored. Following ejection, compacts were transferred to the holder and oriented such that the face proximal to the X-ray source was flush with the holder surface. A schematic of the experimental setup used for transmission PXRD studies is shown in Fig. 2.

### 2.3. Preparation of chlorpropamide compacts

Cylindrical compacts were prepared for all experiments using a Carver single station bench top tablet press (Wabash International, Wabash, IN) equipped with 0.5 in., flat-faced tooling. The applied compression force was maintained at desired magnitudes by means of a hydraulic control system. For consistency in all experiments, the target compact weight totaled 200 mg of material, held at the applied compaction force for 5 s.

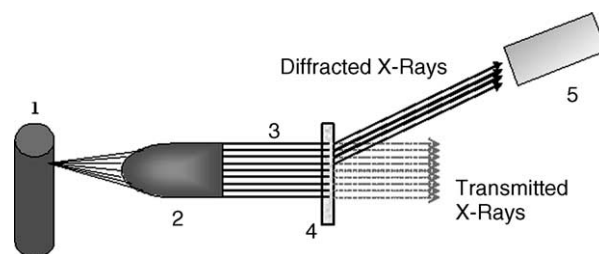


Fig. 2. Schematic figure showing experimental setup for transmission PXRD experiments. X-rays are generated at the Cu anode (1) and collimated through the XOS polycapillary optic (2). Divergence from the optic is less than  $0.25^\circ$ , effectively making the incident X-ray beam (3) parallel. Compact samples are positioned in an aluminum sample holder (4) at a fixed  $\theta$  of  $90^\circ$ . Transmitted X-rays are collected in a detector (5), which rotates through angles of  $2\theta$ .

#### 2.4. Determination of chlorpropamide conversion pressure

Compacts were prepared at various decreasing pressures, each of which was placed in an aluminum transmission PXRD holder and analyzed. Conversion of CPA-A to CPA-C was identified by the appearance of the characteristic 210 reflection for form C at  $15.0^\circ 2\theta$ . Likewise, conversion from CPA-C to CPA-A was monitored using the 102 reflection for CPA-A occurring at  $11.8^\circ 2\theta$ . Transition pressures were identified as those at which a minimum integrated intensity of the characteristic peak for the transformed phase could be reproducibly determined.

#### 2.5. Preparation of a whole compact quantitative standard curve

Compacts having known w/w % compositions of the two CPA forms were prepared. For compacts in which the minority phase represented less than 20% (w/w) of the total compact weight, approximately half of the required majority phase was filled into the die and lightly flattened using the upper punch. The required amount of minority phase was then transferred to the die. Weights less than 10 mg were measured using a Seiko TG/DTA220 SSC/5200 (Seiko Instruments Inc., Japan) as a precision microbalance. The appropriate remaining amount (total target compact weight, 200 mg) of majority phase was transferred to the die, where the entire mixture was compressed at a pressure of 7.0 MPa for a dwell time of 5 s. Upon ejection, compacts were placed in a tared aluminum sample holder, which was subsequently weighed to determine the final compact mass (taking into account all surface material loss due to ejection and transfer). It was assumed that this compact configuration allowed loss of only the majority phase due to edge and surface abrasion, and the relative compositions were adjusted accordingly. For compacts in which the minority phase was greater than 20% (w/w) of the total compact weight, the entire majority phase was first placed into the die and flattened using the face of the upper punch. The entire minority phase was added on top, resulting in a bi-layered compact. Material loss due to abrasion during ejection and transfer was assumed to occur from both phases as a percent commensurate with the volume fraction of each phase within the compact. Triplicate samples at each composition were prepared and analyzed using transmission PXRD. Calibration curves were generated for each phase, plotting the characteristic peak integrated intensity as a function of composition.

#### 2.6. Pressure induced polymorphic transformation of chlorpropamide

Compacts prepared from either pure samples of CPA-A or CPA-C were formed using various applied pressures ranging between 10.0 and 526.7 MPa. The post-compression compact diameter ( $d$ ) and height ( $h$ ) were measured using a digital

micrometer. Assuming a cylindrical geometry, the compact density ( $\rho_{\text{comp}}$ ) was calculated using Eq. (1), where  $m$  is the compact weight:

$$\rho_{\text{comp}} = \frac{4m}{\pi d^2 h} \quad (1)$$

### 3. Results and discussion

#### 3.1. Chlorpropamide as a model compound

The compound selected to demonstrate this quantitative method was the antidiabetic drug chlorpropamide (CPA). Early characterization of CPA polymorphs indicated the existence of at least five distinct crystal forms [11–13]. Most notable among these are two enantiotropes, which have demonstrated a unique and reproducible propensity for phase interconversions during compaction [14–18]. The nomenclature of these two enantiotropes follows that adopted by Simmons et al., in which the low-temperature stable phase is named form A (CPA-A), while its high-temperature stable enantiotrope is named form C (CPA-C) [10].

The PXRD patterns in the range of interest are shown in Fig. 1 for both chlorpropamide phases. The experimentally observed diffraction data are plotted along with calculated patterns generated from the structures for each form. As shown, each phase has a well-separated characteristic diffraction peak, suitable for use in quantitative PXRD studies.

#### 3.2. Determination of conversion pressures

To date, the minimum conversion pressures for both CPA-A and CPA-C remain uncertain. Pressure induced transformations of CPA were originally documented by Ueda et al., who noted that during the preparation of samples for use in intrinsic dissolution studies, CPA-C was transformed to CPA-A when compacted at 2 tons/cm<sup>2</sup> (196 MPa) [14]. Otsuka and co-workers have shown that when compacted at this same pressure, CPA-A will transform to CPA-C [15,16]. While a minimum conversion pressure of 35 MPa has been previously suggested, accurate preparation of a whole compact calibration curve necessitated that a specific conversion pressure be established.

Compacts of pure CPA-A were prepared at pressures ranging from 3.5–35.1 MPa, with subsequent analysis by transmission PXRD. The intensity of the 210 reflection for form C increased with increasing applied pressure (Fig. 3), and indicated that within the detection limit of this instrument, transformation from CPA-A to CPA-C does not occur below pressures of 10.5 MPa. Through observations of the 102 reflection characterizing CPA-A, the same experiments were completed for compacts prepared from pure CPA-C (Fig. 4), yielding the same results. All calibration compacts were, therefore, prepared at pressures

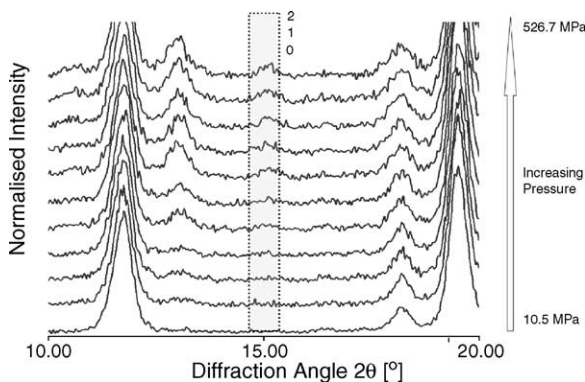


Fig. 3. Waterfall plot of transmission PXRD patterns from compacts prepared from pure CPA-A at various increasing pressures. The box in grey highlights the characteristic 2 1 0 reflection for CPA-C at  $15.0^\circ 2\theta$ .

of 7.0 MPa, enabling sufficient consolidation for analysis without inducing unwanted transformation.

### 3.3. PXRD quantitative considerations for chlorpropamide polymorphs

A reproducible limit of detection for form C in a matrix of form A was determined to be 4.0% (w/w) when evaluated at the 2 1 0 reflection. Similarly, CPA-A was detectable in a matrix of CPA-C using the 1 0 2 reflection at concentrations as low as 2.0% (w/w). This observed difference in detection limits for the two forms is due to the relative intensities of the characteristic peaks for each polymorph (90.24 and 44.94, respectively, for the 1 0 2 and 2 1 0 reflections for forms A and C). Fig. 3 also indicates the emergence of a peak at  $13^\circ 2\theta$ , corresponding to diffraction from CPA-C grains, which has a relative intensity comparable to that of the characteristic reflection for form A. Although useful for qualitative purposes, the  $13.0^\circ 2\theta$  peak corresponds to two CPA-C reflections, making it less suited for quantitative analysis.

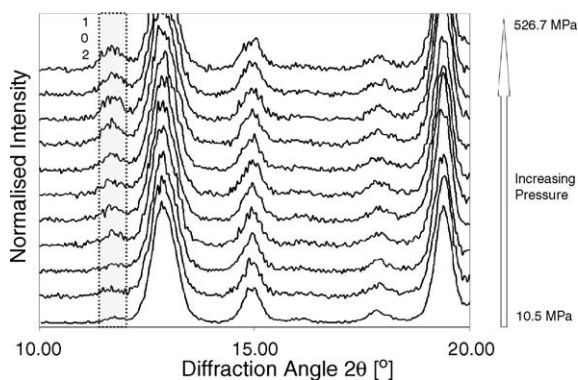


Fig. 4. Waterfall plot of transmission PXRD patterns from compacts prepared from pure CPA-C at various increasing pressures. The box in grey highlights the characteristic 1 0 2 reflection for CPA-A at  $11.8^\circ 2\theta$ .

### 3.4. Preparation of a whole compact quantitative standard curve

Whole compact quantification of multi-phase mixtures can be accomplished using transmission PXRD, by considering the integrated diffraction intensity ( $I_{ij}$ ) of a specific ( $hkl$ ) peak ( $i$ ) occurring at a Bragg angle  $\theta$ , of a given phase ( $j$ ), which can be expressed as:

$$I_{ij} = v_j V \cdot A_j \cdot k_{ij} \quad (2)$$

Here  $v_j$  is the volume fraction of phase  $j$  in the sample having a total volume ( $V$ ),  $A_j$  a correction term for the absorption of X-rays by phase  $j$ , and  $k_{ij}$  is a combination of instrumental and materials constants, listed in Equation (3) [19]:

$$k_{ij} = I_0 \cdot \frac{1 + \cos^2 2\theta}{\sin^2 \theta \cos \theta} \cdot \frac{r_e^2 \lambda^3 M_{ij} H_c}{8\pi R \zeta_j^2} \cdot |F_{\text{obs},ij}|^2 \cdot D_{ij} \quad (3)$$

Above,  $I_0$  is the incident X-ray beam intensity,  $(1+\cos^2 2\theta)/(\sin^2 \theta \cos \theta)$  a combined Lorentz–Polarization correction term,  $r_e$  the classical electron radius,  $\lambda$  the wavelength of the X-ray beam,  $M_{ij}$  the multiplicity of the peak of interest,  $H_c$  the width of the receiving slit at the detector,  $R$  the distance between the sample and the detector,  $\zeta_j$  the volume of a unit cell of phase  $j$ ,  $|F_{\text{obs},ij}|^2$  is the relative structure factor amplitude of a particular peak for phase  $j$ , and  $D_{ij}$  is the Debye–Waller temperature factor:

$$D_{ij} = \exp \left[ -2B \left( \frac{\sin^2 \theta}{\lambda^2} \right) \right] \quad (4)$$

where  $B$  is the isotropic temperature factor for a given crystal structure. Equation (2) can be further simplified by combining terms in Equation (5), which for most experiments are either instrument or material constants, and incorporating them into a general constant,  $K$ .

$$I_{ij} = K v_j \quad (5)$$

The form of Equation (5) shows that for transmission experiments, the integrated intensity of a phase specific peak is directly proportional to the volume fraction of the phase of interest, assuming that the peak is sufficiently isolated such that all diffraction at that angle is accomplished only by the grains of phase  $v_j$  [19].

The extent of transformation during compaction was expected to be less than 20%, thus a set of whole compact calibration data were generated, focusing on the precision of the lower limit data for each phase. The starting points at each end of the curve were initially taken to be the limits of detection. Triplicate compacts were prepared from mechanical mixtures of polymorphs in ratios that increased the minority component by 1% (w/w) up to 10% for CPA-A in C and 15% for CPA-C in A. Intermediate points were also prepared from mixtures of 20%/80%, 30%/70%, 40%/60% and 50%/50%. The resulting calibration data are plotted in Fig. 5. The data corresponding to the 1 0 2 reflection for form A have a slightly lower linear correlation coefficient, biased

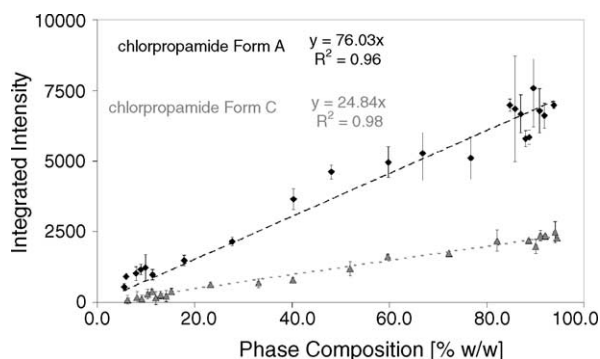


Fig. 5. Whole compact PXRD calibration curve for CPA-A (diamonds) and CPA-C (grey). All compacts were prepared at a constant pressure of 7.0 MPa, resulting in an average  $t = 1.9$  mm and SF = 0.58.

by the mid-points of the curve. This can potentially be explained by the greater tendency of CPA-A to adhere to compaction tooling, slightly reducing the accuracy with which the exact compact composition can be determined. Cao et al. also suggest that the (1 0 2) planes may belong to a potential slip system for CPA-A crystals, which can lead to variability with respect to that peak's intensity and area [3]. The same data variability for central points in the curve based on the 2 1 0 reflection of form C does not occur. CPA-C is easier to handle relative to form A, and adhesion problems were not observed for this polymorph. In addition, computational slip plane analysis was performed according to the method used by Cao et al. [3], which indicated that the (2 1 0) planes are highly unlikely to be involved in mechanical slip, making it inherently less susceptible to variability.

### 3.5. Correction of quantification data for sample thickness and solid fraction

One of the challenges of using PXRD as an analytical tool for whole compact analysis is manifest as diffraction signal attenuation due to effects of consolidation. The necessary adjustments to Equation (2) include expression of the  $V$  and  $A_j$  terms as functions of compact thickness ( $t$ ) and solid fraction (SF) [4].

$$I_{ij} = k_{ij} \cdot v_j C \cdot t \cdot \text{SF} \exp \left[ - \left( \frac{\mu}{\rho} \right) \rho_{\text{cryst},j} \cdot t \cdot \text{SF} \right] \quad (6)$$

Assuming a cylindrical geometry,  $V$  can be expressed as the product of the cross-sectional area ( $C$ ) and the compact thickness ( $t$ ). The SF term accommodates sample porosity inherent to the  $V$  term. A breakdown of  $A_j$  includes a dependence on the mass attenuation coefficient ( $\mu/\rho$ ) and the crystallographic density of phase  $j$  ( $\rho_{\text{cryst},j}$ ). Plotted as a function of either SF or  $t$ , the  $I_{ij}$  for CPA, normalized to its maximum, shows significant signal attenuation as SF approaches 1, and as  $t$  approaches 2 mm (Figs. 6 and 7, respectively). This suggests that simple interpolation of the calibration data (Fig. 5) is valid only when both SF and  $t$  are consistent with those of the calibration samples. Although chemically identical,

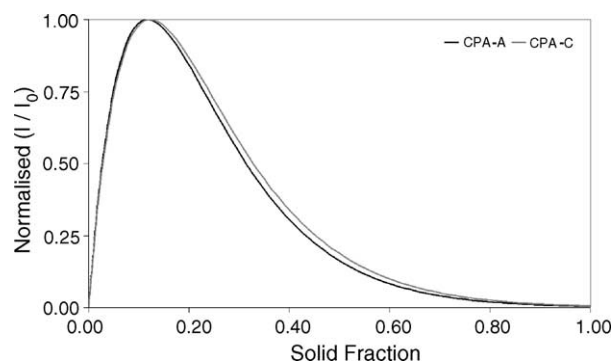


Fig. 6. Signal attenuation of transmission PXRD normalized integrated intensity ( $I/I_0$ ) as a function of solid fraction (SF) for chlorpropamide form A (black) and form C (grey).

compacts prepared at different pressures and dwell times will necessarily have different thicknesses and solid fractions relative to the calibration samples.  $I_{ij}$  must, therefore, be corrected prior to interpolation to accommodate these differences.

Direct measurement of compact thickness allows facile determination of the necessary correction terms provided that  $\rho_{\text{cryst},j}$  of the material is known for the analyte. The solid fraction of any sample can be calculated using Equation (7):

$$\text{SF} = \frac{\rho_{\text{comp}}}{\rho_{\text{cryst}}} \quad (7)$$

For samples containing more than one component,  $\rho_{\text{cryst}}$  is simply the sum of true densities for each phase weighted in terms of their volume fraction, i.e.:

$$\rho_{\text{cryst}} = \sum_j v_j \rho_{\text{cryst},j} \quad (8)$$

For chlorpropamide,  $\rho_{\text{cryst},j}$  is 1.461 g/cm<sup>3</sup> [20] and 1.317 g/cm<sup>3</sup>, respectively, for CPA-A and CPA-C (structure not yet published).

Experiments were conducted in which pure samples of CPA-A and CPA-C were compressed above the transition pressure. The extent of conversion due to compaction

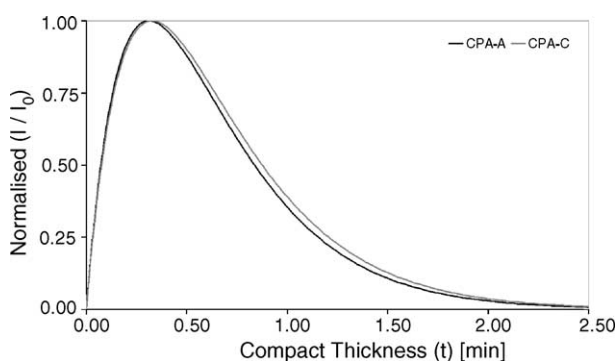


Fig. 7. Signal attenuation of transmission PXRD normalized integrated intensity ( $I/I_0$ ) as a function of compact thickness ( $t$ ) for chlorpropamide form A (black) and form C (grey).

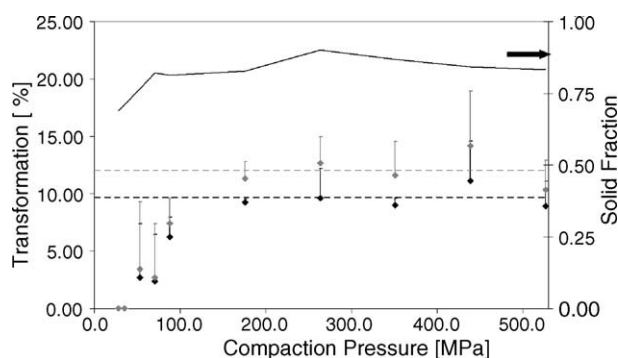


Fig. 8. Transformation of CPA-A with increasing pressure. Data in black are uncorrected for  $t$  and SF, while data in grey are corrected.

pressure was determined by evaluating the characteristic peak of the transformed phase. Assuming insignificant variation in the incident beam intensity over the time course of experimentation, a corrected  $I_{ij}$  for the newly transformed phase (at  $t_2$  and SF<sub>2</sub> relative to the calibration thickness and solid fraction) was calculated using Equation (9):

$$\frac{I_{ij}(t_2, \text{SF}_2)}{I_{ij}(t_1, \text{SF}_1)} = \frac{t_2}{t_1} \cdot \frac{\text{SF}_2}{\text{SF}_1} \exp \left[ \left( \frac{\mu}{\rho} \right) \rho_j \cdot (t_1 \text{SF}_1 - t_2 \text{SF}_2) \right] \quad (9)$$

The mass attenuation coefficient for chlorpropamide was determined by summing  $(\mu/\rho)$  for constituent atoms, weighted by their respective atomic fractions in the molecular formula. For chlorpropamide  $(\mu/\rho) = 29.196 \text{ cm}^2/\text{g}$ .

Application of the signal intensity correction is illustrated in Fig. 8, which shows quantification of the phase transition from CPA-A to CPA-C as a function of pressure. The figure also shows the corresponding change in SF with increasing pressure. As expected from theory, these data confirm that the error associated with direct data interpolation without correction is most significant at the highest compaction pressures, where the difference in  $t$  and SF relative to calibration data is greatest. These data also indicate that small differences in  $t$  and SF, between quantitative and calibration samples (i.e. compacts prepared at pressures similar to those used for calibration samples) are unlikely to introduce significant error into measurement values. Most studies of mechanically activated phase transformations, however, are conducted at pressures much greater than the minimum conversion pressure. The extent to which  $t$  and SF vary relative to the calibration samples will depend on the consolidation properties of the materials. For chlorpropamide, a conversion plateau was observed at pressures greater than 175 MPa. The average extent of transformation over this plateau was initially quantified without correction, resulting in an average of  $9.6 \pm 1.0\%$  ( $n=3$ ). Application of the corrections for  $t$  and SF described in Equation (8) resulted in an average of  $12.0 \pm 1.0\%$  ( $n=3$ ), indicating that the quantitative underestimation for uncorrected chlorpropamide data was approximately 2.4%.

### 3.6. Necessity of quantitative correction and future industrial application

The magnitude by which the chlorpropamide data are corrected is relatively small. Utilization of this type of correction for whole compact phase transformation studies using transmission PXRD is, however, deemed significant, as diffraction data have the potential to vary more substantially depending on the materials used. Consider that for CPA-A the maximum SF reached was 0.85, representing a 19% change in consolidation relative to the initial calibration samples. Fig. 6 illustrates that the changes in  $I_{ij}$  with increasing SF are relatively small over the range of 0.75–1.0, thus the magnitude by which the data are corrected is as expected. If, however, calibration compacts are prepared at much lower SF (i.e. between 0.4 and 0.5), the decrease in  $I_{ij}$  and the consequential increase in quantitative error becomes more and more significant. Situations such as these will depend on the material; where the properties of the calibration compacts will be determined by the compactability of a solid, as well as the minimum conversion pressure for a given set of polymorphs. As a theoretical example, consider a material having sufficient compactability that low-pressure PXRD calibration samples are prepared at SF=0.40. Assuming the same instrument and materials constants used above, and a consolidation limit between 0.85 and 0.90 (typical of organic solids), failure to correct for signal attenuation at high pressures would result in a quantitative error between 26 and 33%.

## 4. Conclusions

Non-destructive, quantification of binary mixture compacts can be accomplished using transmission PXRD methods provided that the incident X-radiation is sufficiently high. This technique enables direct quantification of phase transformations induced by compression, without requiring physical manipulation of samples, which could potentially cause further transitions. Evaluation of data prepared at different stress states relative to the calibration data requires a simple mathematical correction to account for signal attenuation due to differences in sample thickness and solid fraction. Application of this correction illustrated that direct interpolation of pressure-induced transformations of chlorpropamide polymorphs from transmission PXRD data underestimated quantitative values by 2.4%. The magnitude of this error depends largely on the compaction properties of the materials being studied, becoming much greater for compacts prepared at high pressures depending on the  $t$  and SF of the initial calibration samples.

## Acknowledgement

The authors would like to thank the generous funding provided by Pfizer Global Research and Development.

## References

- [1] S. Byrn, R. Pfeiffer, M. Ganey, C. Hoiberg, G. Poochikian, *Pharm. Res.* 12 (1995) 945–954.
- [2] R. Jenkins, R.L. Snyder, *Introduction to X-Ray Powder Diffractometry*, John Wiley and Sons Inc., New York, 1996.
- [3] W. Cao, S. Bates, G.E. Peck, P.L.D. Wildfong, Z. Qiu, K.R. Morris, *J. Pharm. Biomed. Anal.* 30 (2002) 1111–1119.
- [4] W. Cao, M.P. Mullarney, B.C. Hancock, S. Bates, K.R. Morris, *J. Pharm. Sci.* 92 (2003) 2345–2353.
- [5] M. Otsuka, N. Kaneniwa, *Chem. Pharm. Bull.* 32 (1984) 1071–1079.
- [6] T.P. Shakhshneider, V.V. Boldyrev, *Drug Dev. Ind. Pharm.* 19 (1993) 2055–2067.
- [7] J. Font, J. Muntasell, E. Cesari, *Res. Bull.* 32 (1997) 1691–1696.
- [8] T. Yamanoi, H. Nakazawa, *J. Appl. Cryst.* 33 (2000) 389–391.
- [9] B.D. Cullity, S.R. Stock, *Elements of X-Ray Diffraction*, third ed., Prentice-Hall, Upper Saddle River, 2001.
- [10] D.L. Simmons, R.J. Ranz, N.D. Gyanchandani, *Can. J. Pharm. Sci.* 8 (1973) 125–127.
- [11] A. Burger, *Sci. Pharm.* 43 (1975) 152–161.
- [12] A. Burger, *Acta Pharm. Technol.* 28 (1982) 152–161.
- [13] S.S. Al-Saieq, G.S. Riley, *Pharm. Acta Helv.* 57 (1982) 8–11.
- [14] H. Ueda, N. Nambu, T. Nagai, *Chem. Pharm. Bull.* 32 (1984) 244–250.
- [15] M. Otsuka, T. Matsumoto, N. Kaneniwa, *J. Pharm. Pharmacol.* 41 (1989) 665–669.
- [16] T. Matsumoto, N. Kaneniwa, S. Higuchi, M. Otsuka, *J. Pharm. Pharmacol.* 43 (1991) 74–78.
- [17] M. Otsuka, T. Matsumoto, S. Higuchi, K. Otsuka, N. Kaneniwa, *J. Pharm. Sci.* 84 (1995) 614–618.
- [18] M.M. DeVilliers, D.E. Wurster, *Acta Pharm.* 49 (1999) 79–88.
- [19] L.S. Zevin, G. Kimmel, *Quantitative X-Ray Diffractometry*, Springer, New York, 1995.
- [20] C.H. Koo, S.I. Cho, Y.H. Yeon, *Arch. Pharmacol. Res.* 3 (1980) 37–49.